

New Charge Transfer Luminescent Polymetallic Complexes of Rhodium(III), Iridium(III), and Ruthenium(II) with the Bridging Ligand 1,4,5,8,9,12-Hexaazatriphenylene

I. Ortmans, P. Didier, and A. Kirsch-De Mesmaeker^{†,*}

Université Libre de Bruxelles, Chimie Organique Physique, CP 160/08, 50 av.
F. D. Roosevelt, 1050 Bruxelles, Belgium

Received July 14, 1994[⊗]

New emitting binuclear $(\text{Rh})_i-(\text{Ru})_{2-i}$ ($i = 1, 2$), $(\text{Ir})-(\text{Ru})$, and trinuclear $(\text{Rh})_i-(\text{Ru})_{3-i}$ ($i = 1, 2, 3$) complexes assembled by the trischelating bridging ligand HAT (1,4,5,8,9,12-hexaazatriphenylene), have been synthesized. Their characterization by mass spectrometry (FAB and electrospray) is in accordance with their expected structure, where $\text{Rh}(\text{PPY})_2^+$ (or $\text{Ir}(\text{PPY})_2^+$) and $\text{Ru}(\text{BPY})_2^{2+}$ correspond to the building blocks (PPY is the ortho-C-deprotonated form of 2-phenylpyridine and BPY is 2,2'-bipyridine). The HPLC data of these polymetallic compounds reveal that the *trimetallic homo-* and *heteronuclear* complexes are not stable under the chromatographic conditions and in some organic solvents. Therefore, the electrochemical and photophysical data are given only for the bimetallic compounds, stable under these conditions. Under electrochemical oxidation, the bimetallic Rh(III) complex shows one irreversible wave in the accessible potential range, while the heteronuclear Rh(III)–Ru(II) and Ir(III)–Ru(II) compounds exhibit an irreversible process followed by a reversible wave. For the bimetallic (homo- and heteronuclear) complexes, the first reduction wave involves a HAT-centered π^* orbital. On the basis of the electrochemical, luminescence and resonance Raman data, the lowest electronic transitions are CT (charge transfer) transitions involving the bridging HAT. These transitions have an MLCT (metal to ligand charge transfer) type for the Ru(II) moiety and a SBLCT (σ -bond to ligand charge transfer) character for the Rh(III) unit; in the case of the Ir(III) moiety there is a strong admixture of SBLCT and MLCT character. An energy transfer would take place from the Ru–HAT ³MLCT state towards the Ir–HAT ³SBLCT (mixed with ³MLCT character) in the Ir(III)–Ru(II) compound. For the Rh(III)–Ru(II) complex the nature of the luminescent excited state (Ru–HAT ³MLCT or Rh–HAT ³SBLCT) cannot be unambiguously determined.

Introduction

Ru(II)–polypyridyl complexes have been the subject of many investigations resulting in a fairly good understanding of their electrochemical and photophysical properties.¹ In recent years the research in this area has been extended from the study of “simple” monometallic compounds to the development of polymetallic, supramolecular systems showing varied functions at the different metal centers.² Some polynuclear edifices have been prepared in view of their optical activity³ or have been exploited as new photosensitizers;⁴ others have been considered as models for the study of photoinitiated intramolecular electron⁵ or energy⁶ transfer. For recent reviews in this area, see ref 2a.

In our laboratory, for several years,⁷ we have also investigated the possibility of designing new polymetallic complexes for various applications. We have used a symmetric polyazaaromatic trischelating bridging ligand, the 1,4,5,8,9,12-hexaazatriphenylene (HAT).⁸ The electrochemical and photophysical properties of the Ru(II) homonuclear polymetallic complexes built with this HAT ligand, such as the $[\text{Ru}(\text{BPY})_2]_n\text{HAT}^{2n+}$ (n

$= 1, 2, 3$) (BPY = 2,2'-bipyridine) and the corresponding heteroleptic complexes where some of the ancillary BPY ligands are replaced by PHEN (PHEN = 1,10-phenanthroline), TAP (TAP = 1,4,5,8-tetraazaphenanthrene), or HAT ligands, have been extensively examined in our laboratory;^{9,10} the data indicate a significant interaction between the metal centers through the

* Author to whom correspondence should be addressed.

[†] Director of Research at the National Fund for Scientific Research (Belgium).

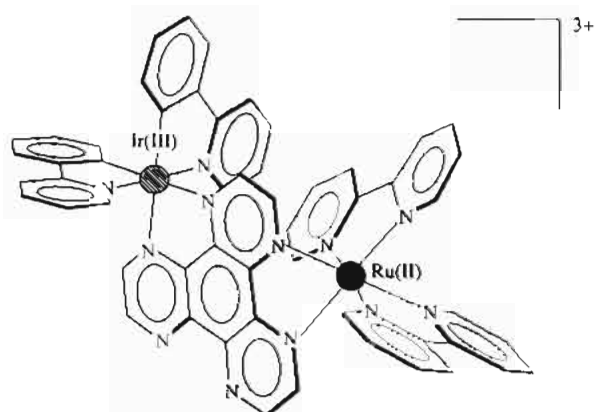
[⊗] Abstract published in *Advance ACS Abstracts*, June 15, 1995.

- (1) (a) Meyer, T. J. *Pure Appl. Chem.* **1986**, *58*, 1193. (b) Kalyanasundaram, K. *Coord. Chem. Rev.* **1982**, *46*, 159. (c) Juris, A.; Balzani, V.; Barigelli, F.; Campagna, S.; Belsler, P.; Von Zelewsky, A. *Coord. Chem. Rev.* **1988**, *84*, 85.
- (2) (a) Balzani, V.; Scandola, F. *Supramolecular Photochemistry*; Ellis Horwood: Chichester, England, 1991. (b) Scandola, F.; Bignozzi, C. A.; Chiorboli, C.; Indelli, M. T.; Rampi, M. A. *Coord. Chem. Rev.* **1990**, *97*, 299.
- (3) Sudhakar, A.; Katz, T. J.; Bing-Wei Yang *J. Am. Chem. Soc.* **1986**, *108*, 2790.
- (4) Hunziker, M.; Ludi, A. *J. Am. Chem. Soc.* **1977**, *99*, 7370.

- (5) (a) Bignozzi, C. A.; Roffia, S.; Scandola, F. *J. Am. Chem. Soc.* **1985**, *107*, 1644. (b) Duesing, R.; Tapolsky, G.; Meyer, T. J. *J. Am. Chem. Soc.* **1990**, *112*, 5378. (c) Ogawa, M. Y.; Wishart, J. F.; Young, Z.; Miller, J. R.; Isied, S. S. *J. Phys. Chem.* **1993**, *97*, 11456. (d) De Cola, L.; Balzani, V.; Barigelli, F.; Flamigni, L.; Belsler, P.; von Zelewsky, A.; Frank, M.; Vögtle, F. *Inorg. Chem.* **1993**, *32*, 5228. (e) Yoshimura, A.; Nozaki, K.; Ikeda, N.; Ohno, T. *J. Am. Chem. Soc.* **1993**, *115*, 7521.
- (6) (a) Schmehl, R. H.; Auerbach, R. A.; Wacholtz, W. F. *J. Phys. Chem.* **1988**, *92*, 6202. (b) Scandola, F.; Indelli, M. T.; Chiorboli, C.; Bignozzi, C. A. *Top. Curr. Chem.* **1990**, *158*, 73. (c) Barigelli, F.; Flamigni, L.; Balzani, V.; Collin, J.-P.; Sauvage, J.-P.; Sour, A.; Constable, E. C.; Cargill Thompson, A.M.W. *J. Chem. Soc., Chem. Commun.* **1993**, 943. (d) Vögtle, F.; Frank, M.; Nieger, M.; Belsler, P.; von Zelewsky, A.; Balzani, V.; Barigelli, F.; De Cola, L.; Flamigni, L. *Angew. Chem., Int. Ed. Engl.* **1993**, *32*, 1643. (e) Schoonover, J. R.; Gordon, K. C.; Argazzi, R.; Woodruff, W. H.; Peterson, K. A.; Bignozzi, C. A.; Dyer, R. B.; Meyer, T. J. *J. Am. Chem. Soc.* **1993**, *115*, 10996. (f) Wang, Y.; Schanze, K. S. *Inorg. Chem.* **1994**, *33*, 1354.
- (7) Masschelein, A.; Kirsch-De Mesmaeker, A.; Verhoeven, C.; Nasielski-Hinkens, R. *Inorg. Chim. Acta* **1987**, *129*, L13.
- (8) (a) Nasielski-Hinkens, R.; Benedek-Vamos, M.; Maetens, D.; Nasielski, J. *J. Organomet. Chem.* **1981**, *217*, 178. (b) Nasielski, J.; Moucheron, C.; Verhoeven, C.; Nasielski-Hinkens, R. *Tetrahedron Lett.* **1990**, *31*, 2573.
- (9) (a) de Buyl, F.; Kirsch-De Mesmaeker, A.; Tossi, A.; Kelly, J. M. *J. Photochem. Photobiol. A: Chem.* **1991**, *60*, 27. (b) Jacquet, L.; Kirsch-De Mesmaeker, A. *J. Chem. Soc., Faraday Trans.* **1992**, *88(17)*, 2471.
- (10) (a) Vanhecke, F.; Heremans, K.; Kirsch-De Mesmaeker, A.; Jacquet, L.; Masschelein, A. *J. Raman Spectrosc.* **1989**, *20*, 617. (b) Kirsch-De Mesmaeker, A.; Jacquet, L.; Masschelein, A.; Vanhecke, F.; Heremans, K. *Inorg. Chem.* **1989**, *28*, 2465.

HAT bridge. In order to investigate the heterometallic Rh(III)–Ru(II) and Ir(III)–Ru(II) compounds, where the Rh for example could possibly play the role of catalytic metal center after reduction,¹¹ we first examined the properties of the monometallic Rh–HAT and Ir–HAT building blocks.¹² The syntheses of these units have not been possible with BPY or PHEN as ancillary ligands, and required the presence of two strong σ -donor orthometalating PPY ligands (HPPY = 2-phenylpyridine), in order to compensate the π -deficient character of the HAT ligand. Interestingly, contrary to the previously studied Rh(PPY)₂BPY⁺ compound, which exhibits a π – π^* localized emission,¹³ the Rh–(PPY)₂HAT⁺ complex shows a room temperature luminescence originating from a state of charge transfer to the HAT, which has been described in terms of a SBLCT (σ -bond to ligand charge transfer) excited state.^{12,14} Some supplementary complexity is observed for Ir(PPY)₂HAT⁺: in this case, a strong admixture of SBLCT and MLCT (metal to ligand charge transfer) behavior results in two closely spaced excited states, both with a charge transfer to the accepting HAT π^* orbital.

These luminescence features brought by the HAT ligand made mixed metal Rh(III)–Ru(II) and Ir(III)–Ru(II) complexes (such as A) interesting for the study of photoinduced intramolecular



A: $[\text{Ir}(\text{PPY})_2]\text{HAT}[\text{Ru}(\text{BPY})_2]^{3+}$

processes. Recently, a study published by another laboratory on bimetallic Rh–Ru and Rh–Rh complexes based on a triazole bridge¹⁵ has shown that the Rh component in the homobimetallic complex has an emission originating from a ligand-centered excited state, as observed for the monometallic compound Rh–(PPY)₂BPY⁺. This example stresses again that the Rh–HAT unit behaves differently concerning the luminescence properties.

This contribution focuses in a first stage on one of the major problems encountered in the study of polymetallic compounds, i.e. characterization of the polynuclear edifices and detection

of impurities or decomposition products. It is indeed essential to establish not only the structure but also the purity of the samples before performing luminescence experiments. Especially in the case of polymetallic complexes, traces of monometallic impurities characterized by higher emission quantum yields can significantly modify the luminescence features. The FAB,¹⁶ electrospray, and HPLC results allow us to report in the second part of this work the electrochemical and photo-physical properties of the bimetallic Rh–Rh, Rh–Ru, and Ir–Ru compounds for which unambiguous proofs of purity are obtained.

Experimental Section

A. Syntheses. The polymetallic complexes discussed in this paper were synthesized and purified following a previously described procedure.¹⁶ The homonuclear $[\text{Rh}(\text{PPY})_2]\text{HAT}^{2+}$ and $[\text{Rh}(\text{PPY})_2]\text{HAT}^{3+}$ compounds were prepared from the dichloro-bridged dimer $[\text{Rh}(\text{PPY})_2\text{Cl}]_2$ reacting with the HAT ligand in a dichloromethane/methanol (1:1) mixture; the purification was performed by exclusion chromatography on a Sephadex LH-20 column with water as eluent. The purity was checked at this stage by TLC with DMF/H₂O (1:1; NH₄Cl 1 M). Reaction of the $[\text{Ru}(\text{BPY})_2]\text{HAT}^{2+}$ and $[\text{Ru}(\text{BPY})_2]\text{HAT}^{4+}$ with the appropriate dichloro-bridged dimer in dichloromethane/methanol (1:1) resulted in formation of the heteronuclear complexes $[\text{Rh}(\text{PPY})_2]\text{HAT}[\text{Ru}(\text{BPY})_2]^{3+}$, $[\text{Ir}(\text{PPY})_2]\text{HAT}[\text{Ru}(\text{BPY})_2]^{3+}$, $[\text{Rh}(\text{PPY})_2]\text{HAT}[\text{Ru}(\text{BPY})_2]^{4+}$, and $[\text{Rh}(\text{PPY})_2]\text{HAT}[\text{Ru}(\text{BPY})_2]^{5+}$. These compounds were purified on a cation exchange Sephadex SP-C25 column with aqueous NaCl as eluent; the fractions containing the desired compound were treated with CH₂Cl₂ saturated in KPF₆ in order to extract the complex under the form of the PF₆ salt. Purity was checked by TLC, with DMF/H₂O (1:1; NH₄Cl 1 M).

B. Characterization by Mass Spectrometry. All the polymetallic compounds mentioned above were identified by FAB mass spectrometry.¹⁶ Complementary analyses were performed by electrospray mass spectrometry (ESMS), on a VG BioQ tri-quadrupole mass spectrometer (VG BioTech Ltd. Altrincham, U.K.). The mass spectrometer scanned from m/z 0 to m/z 4000 (scanning rate = 100 m/z units per second). Resolution was 700 at 10% valley (lower than FAB resolution). The bi- and trimetallic samples were dissolved in dichloromethane and the resulting solutions (10 μL , about 10–50 μM) were introduced into the ion source at a rate of 5 $\mu\text{L min}^{-1}$. The electrostatic spray ion source was operated at atmospheric pressure at 3000 V and source temperature was 50 °C. The extraction cone voltage (V_c) was 10 V; higher V_c values (until 70 V) were also used to perform fragmentation studies. These ESMS analyses were carried out in the laboratory of Professor A. van Dorsselaer, University L. Pasteur, Strasbourg, France.

C. HPLC. HPLC analyses were performed with a Waters equipment on a C18 inverted phase column (Waters, $\mu\text{Bondapak}$ 10 μm , 10 mm \times 8 mm cartridge). The elution program consisted in a H₂O (pH = 2.5)/CH₃OH linear gradient (0–100% methanol in 15 min). Detection was performed by a UV–visible diode-array spectrometer, from 220 to 600 nm. Flow rate was maintained at 2 mL/min. All the analyses were carried out in the laboratory of Professor J. Lhomme, University J. Fourier, Grenoble, France.

D. Cyclic Voltammetry. Cyclic voltammetry was performed in a one-compartment cell which consisted in a platinum disk working electrode (approximate area = 20 mm²), a platinum wire counter electrode, and a saturated calomel electrode (SCE) as reference electrode (Radiometer K701). The potential of the working electrode was controlled by a home-made potentiostat. Scan rates (0.01 to 1 V s⁻¹) and scanning range were produced by a frequency generator (Philips PM 5168) and monitored by a Telequipment D 1011 oscilloscope. All the cyclic voltammograms were recorded in acetonitrile (Aldrich 99.8%), distilled twice over P₂O₅ and CaH₂. The concentration of the complexes was maintained at 1 mM and each solution contained 0.1 M of tetrabutylammonium hexafluorophosphate (Fluka puriss.) as supporting electrolyte. Before each measurement the samples were purged by nitrogen.

- (11) (a) Kirch, M.; Lehn, J.-M.; Sauvage, J.-P. *Helv. Chim. Acta* **1979**, *62*, 1345. (b) Chan, S.-F.; Chou, M.; Creutz, C.; Matsubara, T.; Sutin, N. *J. Am. Chem. Soc.* **1981**, *103*, 369. (c) Vogler, L. M.; Scott, B.; Brewer, K. J. *Inorg. Chem.* **1993**, *32*, 898. (d) Indelli, M. T.; Bigozzi, C. A.; Harriman, A.; Schoonover, J. R.; Scandola, F. *J. Am. Chem. Soc.* **1994**, *116*, 3768.
- (12) Didier, P.; Ortmans, I.; Kirsch-De Mesmaeker, A.; Watts, R. *J. Inorg. Chem.* **1993**, *32*, 5239.
- (13) (a) Wilde, A. P.; King, K. A.; Watts, R. *J. Phys. Chem.* **1991**, *95*, 629. (b) Frei, G.; Zilian, A.; Raselli, A.; Güdel, H. U. *Inorg. Chem.* **1992**, *31*, 4766. (c) Miki, H.; Shimada, M.; Azumi, T.; Brozik, J. A.; Crosby, G. A. *J. Phys. Chem.* **1993**, *97*, 11175. (d) Giesbergen, C.; Glasbeek, M. J. *J. Phys. Chem.* **1993**, *97*, 9942. (e) Colombo, M. G.; Brunold, T. C.; Riedener, T.; Güdel, H. U.; Förtsch, M.; Bürgi, H.-B. *Inorg. Chem.* **1994**, *33*, 545.
- (14) (a) Djurovitch, P. I.; Safir, A.; Keder, N.; Watts, R. *J. Coord. Chem. Rev.* **1991**, *111*, 201. (b) Djurovitch, P. I.; Watts, R. *J. Inorg. Chem.* **1993**, *32*, 4681.
- (15) van Diemen, J. H.; Hage, R.; Haasnoot, J. G.; Lempers, H. E. B.; Reedijk, J.; Vos, J. G.; De Cola, L.; Barigelli, F.; Balzani, V. *Inorg. Chem.* **1992**, *31*, 3518.

- (16) Didier, P.; Jacquet, L.; Kirsch-De Mesmaeker, A.; Hucber, R.; van Dorsselaer, A. *Inorg. Chem.* **1992**, *31*, 4803.

Table 1. Main Peaks Observed in the ES (Electrospray) MS Spectra^a of the Bimetallic and Trimetallic Complexes

complex	mass ^b	[M - P ⁻] ⁺ ^c	[M - 2P ⁻] ²⁺ ^c	[M - 3P ⁻] ³⁺ ^c	other main peaks ^c
Bimetallic Compounds					
[Rh(Py) ₂] ₂ H ²⁺ (P ⁻) ₂	1346.7	1201.3 ⁴⁰ (1201.1)	528.1 ¹⁰⁰ (528.1)		
[Rh(Py) ₂] ₂ H[Ru(B) ₂] ³⁺ (P ⁻) ₃	1493.8	1348.5 ⁵⁵ (1349.0)	602.2 ¹⁰⁰ (602.1)		
[Ir(Py) ₂] ₂ H[Ru(B) ₂] ³⁺ (P ⁻) ₃	1583.2	1438.5 ²⁰ (1439.1)	646.8 ¹⁰⁰ (647.1)		
Trimetallic Compounds					
[Rh(Py) ₂] ₂ H[Ru(B) ₂] ⁴⁺ (P ⁻) ₄	2050.1		879.6 ¹⁰⁰ (880.1)		[[Rh(Py) ₂] ₂ H[Ru(B) ₂] ³⁺ (P ⁻) ₂] ²⁺ , 602.3 ¹⁰ (602.1)
[Rh(Py) ₂] ₂ H[Ru(B) ₂] ⁵⁺ (P ⁻) ₅	2197.2		953.1 ¹⁰⁰ (954.0)	587.5 ²⁵ (587.7)	[[Ru(B) ₂] ₂ H ⁴⁺ (P ⁻) ₂] ²⁺ , 675.5 ³⁵ (676.0); [[Ru(B) ₂] ₂ H ⁴⁺ P ⁻] ³⁺ , 402.9 ⁵ (402.4)
[Rh(Py) ₂] ₃ H ³⁺ (P ⁻) ₃	1903.0	1757.9 ⁵⁰ (1757.1)	805.9 ¹⁰⁰ (806.1)	489.7 ¹⁰ (489.1)	[[Rh(Py) ₂] ₂ H ²⁺ P ⁻] ⁺ , 1201.2 ³⁵ (1201.1); [Rh(Py) ₂] ₂ H ²⁺ , 528.7 ³⁰ (528.1)

^a Cone voltage = 10 V, positive mode. ^b Calculated chemical mass. ^c *m/z* observed for the largest isotopic peaks with relative intensities in superscript and calculated values for *m/z* in parentheses. Key: H, 1,4,5,8,9,12-hexaazatriphenylene; B, 2,2'-bipyridine; Py, 2-phenylpyridine; P⁻, PF₆⁻.

E. Spectroscopy. Absorption spectra were monitored with a Hewlett-Packard HP 8452A UV-visible diode array spectrophotometer equipped with a Hewlett-Packard HP Vectra QS16 computer. The molar extinction coefficients of the complexes were determined by Ruthenium and Rhodium titration by plasma emission spectroscopy with a Spectrometric Spectrospan IV instrument.

Excitation spectra were recorded with a Shimadzu RF-5001PC spectrofluorimeter equipped with a Hamamatsu R928 photomultiplier tube and connected to a Compaq ProLinea 4/25s computer. Correction factors for the instrumental characteristics were determined with a P/N 204-07550 spectrum correction attachment, using a concentrated solution of Rhodamine B in ethylene glycol (8 mg/mL) as quantum counter.

Raman and resonance Raman experiments were performed with a Spex Triplemate instrument equipped with an optical multichannel analyzer (OMA III, EG&G Princeton Applied Research). Excitation of the aqueous solutions in quartz capillaries was performed with a continuous Argon laser (Spectra Physics 2020). These experiments were carried out in the laboratory of Professor J. McGarvey, Queen's University of Belfast.

Emission spectra were recorded with a modified Applied Photo-physics laser kinetic spectrometer, equipped with a Hamamatsu R928 photomultiplier tube and with a 300 W Xenon arc lamp (ORC XM 300-5) as emitting source.

Emission lifetimes were measured with the same laser kinetic apparatus by exciting the samples at 354 nm with a Nd-YAG pulsed laser. Emitted light as a function of time was detected with a R928 Hamamatsu photomultiplier tube whose output was applied to a digital oscilloscope (Hewlett Packard HP 54200A) connected through an IEEE 488 interface to a HP 9816 S computer. Signals were averaged over 16 shots and corrected for baseline. Kinetic analyses of the decays were achieved by using nonlinear least-squares regressions derived from a modified Marquardt's algorithm.¹⁷

Results

Syntheses. The homonuclear Rh complexes, with two and three Rh(III) metal centers, were obtained by condensing two or three Rh(PPY)₂⁺ units, produced from the reactive dichloro-bridged dimer [Rh(PPY)₂Cl]₂, on the chelating bridging HAT. For the heterobimetallic compounds, the syntheses were performed from the mononuclear Ru(BPY)₂HAT²⁺ complex to which one equivalent of the Rh(III) or Ir(III) unit was added in order to obtain the Rh-Ru and Ir-Ru compounds. The heterotrimetallic complexes Rh₂-Ru and Rh-Ru₂ were prepared from the mononuclear or binuclear Ru(II) complexes reacting with 2 or 1 equiv of Rh(III) units, respectively.

All the samples were chromatographed several times for purification as described in the experimental section and their purity was checked by TLC. Despite these purification procedures, the first results reported several years ago¹⁸ on the

emissions of the so-obtained hetero-bi- and trinuclear Rh-Ru complexes suggested the presence of traces of impurities. This problem is developed below.

Characterization. The characterization of polymetallic complexes raises many problems. Indeed the NMR spectra of these compounds are too complex to be interpreted without ambiguity so that they do not furnish clear-cut data on the structure of the polymetallic edifice. The complexity of the spectra originates namely from the presence of diastereoisomers which multiply the signals of the different ligands. For example for [Rh(PPY)₂]₂HAT[Ru(BPY)₂]³⁺, the 38 protons have to be multiplied by two to account for the diastereoisomers (ΛΛ/ΔΔ and ΛΔ), which leads to 76 aromatic peaks. Therefore the complexes presented in this paper need to be characterized by other techniques than NMR. In this regard, FAB and electrospray mass spectrometry (ESMS) constitute up to now excellent methods for unambiguous characterization of the polymetallic complexes, especially if the solutions are also analyzed by HPLC in order to detect possible impurities (see below).

The spectra obtained by FAB mass spectrometry for the whole series of complexes¹⁶ were in good accordance with the expected products. However as fragments are always observed in FAB, the presence of mono- or bimetallic impurities that correspond to the mass of the observed fragments in the bi- or trimetallic samples cannot be excluded with certainty. In order to further characterize the compounds of this study, ES mass spectra were also recorded and analyzed. If conditions can be found for which only the parent peak or pseudomolecular fragment ions are present, this method constitutes a proof not only for the mass of the polymetallic complex but also for its purity, in complement to the HPLC data. Additional fragmentation studies performed in other ES conditions should provide proof of the structure.

The ESMS data recorded at low cone voltage (*V*_c = 10 V) for the bi- and trimetallic compounds are summarized in Table 1. All the corresponding spectra are characterized by several isotopic clusters covering up to 10 *m/z* units, due to the presence of the numerous metallic isotopes; the theoretical isotopic distributions have been calculated and are in good agreement with the experimental isotopic profiles observed at enhanced resolution. The ES data have been interpreted using the largest isotopic peak for each isotopic cluster, this peak being calculated by using the atomic mass of the most abundant isotope for each element.

The ES mass data obtained for the bimetallic compounds confirm the proposed structure. Moreover as concluded from

(17) Demas, J. N. *Excited State Lifetime Measurements*; Academic Press: New York, 1983.

(18) Kirsch-De Mesmaeker, A.; Didier, P.; Ortmans, I. Presented at the 9th Symposium on Photochemistry and Photophysics of Coordination Compounds, Fribourg, Switzerland, 14-19 July 1991.

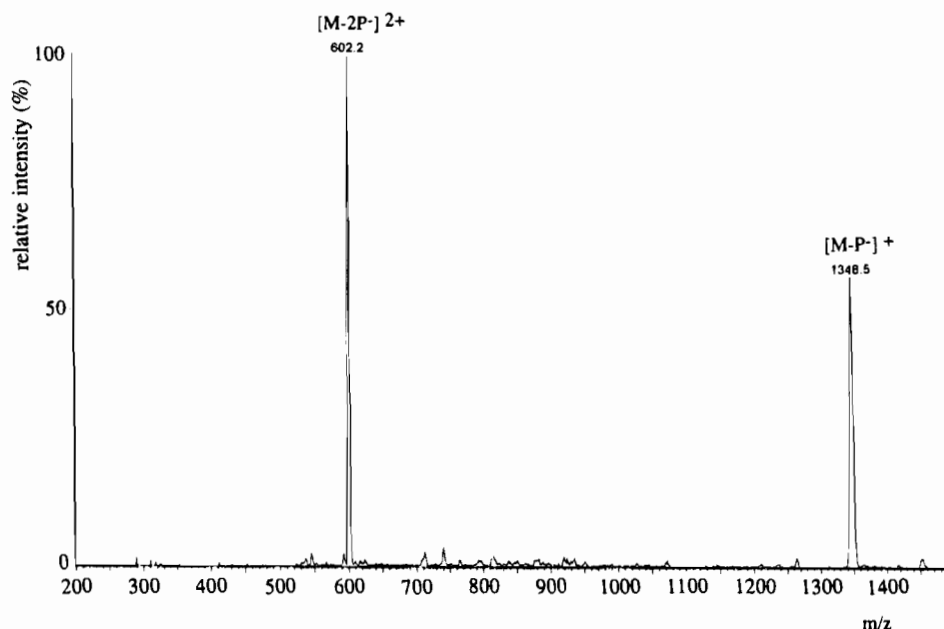


Figure 1. Positive ion ES (electrospray) mass spectrum of the heterobimetallic $[\text{Rh}(\text{PPY})_2]\text{HAT}[\text{Ru}(\text{BPY})_2]^{3+}$ complex recorded at low accelerating potential ($V_c = 10$ V); $\text{P}^- = \text{PF}_6^-$.

the data obtained at low cone voltage, no monometallic impurities are detected in the analyzed samples (see Table 1: no other main peaks). Figure 1 presents the ES mass spectrum ($V_c = 10$ V) recorded for the heterobimetallic Rh–Ru compound: a fragment ion at $m/z = 1348.5$ (calculated $m/z = 1349.0$), bearing a single positive charge, corresponds to the loss of one negatively charged PF_6^- counterion; a second loss of PF_6^- produces the major ion of the spectrum at $m/z = 602.2$ (calculated $m/z = 602.1$). For increased values of the cone voltage ($V_c \geq 30$ V), additional fragment ions corresponding to $\text{Rh}(\text{PPY})_2^+$ at $m/z = 411.9$ (calculated $m/z = 411.0$) and to $[\text{Ru}(\text{BPY})_2\text{HAT}^{2+}\text{PF}_6^-]^+$ at $m/z = 792.7$ (calculated $m/z = 793.1$) are observed in the ES spectra of the heterobimetallic Rh–Ru (data not shown); these fragmentations give additional support to the proposed structure for this compound. A similar fragmentation behavior ($V_c \geq 30$ V) is observed for the two other binuclear compounds, i.e. Ir–Ru ($[\text{Ir}(\text{PPY})_2]^+$ at $m/z = 501.1$, calculated $m/z = 501.1$; $[\text{Ru}(\text{BPY})_2\text{HAT}^{2+}\text{PF}_6^-]^+$ at $m/z = 792.8$, calculated $m/z = 793.1$) and Rh–Rh ($\text{Rh}(\text{PPY})_2^+$ at $m/z = 411.9$, calculated $m/z = 411.0$; $\text{Rh}(\text{PPY})_2\text{HAT}^+$ at $m/z = 645.5$, calculated $m/z = 645.1$).

For the trimetallic compounds Rh_2 –Ru, Rh– Ru_2 and Rh_3 , the ES results indicate very clearly the presence of the expected complexes: in each case the major fragment ion observed at reduced cone voltage originates from the loss of two negatively charged PF_6^- ions ($\text{M} - 2\text{P}^-$). For Rh– Ru_2 and Rh_3 , a triply charged ion corresponding to the loss of three PF_6^- ions is also observed ($\text{M} - 3\text{P}^-$), while the spectrum obtained with Rh_3 is further characterized by a peak associated to the loss of one PF_6^- ($\text{M} - \text{P}^-$).¹⁹ The ES data recorded at low cone voltage seem to reveal also the presence of decomposition product or impurity in all the trimetallic samples. This product corresponds in each case to a bimetallic compound which would be generated

by dechelation of a $\text{Rh}(\text{PPY})_2^+$ unit. Despite the presence of bimetallic impurities, the expected trimetallic compounds remain the major constituents of the analyzed samples. Moreover fragmentation patterns observed at higher voltage values ($V_c \geq 30$ V) confirm the proposed structures for these complexes.

Tests of Purity and Stability. As TLC did not allow the detection of impurities and as HPLC gave satisfactory results during our previous studies on polymetallic homonuclear Ru(II) complexes,^{9b} we used this method for the present study, in complement to the ESMS analyses. No impurities were detected in the samples of the homonuclear $[\text{Rh}(\text{PPY})_2]\text{HAT}^{2+}$ complex, in accord with the ES data. In contrast the analyzed samples of $[\text{Rh}(\text{PPY})_2]\text{HAT}[\text{Ru}(\text{BPY})_2]^{3+}$ and $[\text{Ir}(\text{PPY})_2]\text{HAT}[\text{Ru}(\text{BPY})_2]^{3+}$ contained approximately 5% impurities corresponding to the monometallic complex $[\text{Ru}(\text{BPY})_2]\text{HAT}^{2+}$ and to the dichloro-bridged dimer. If only a few milligrams of these samples were chromatographed on a second Sephadex column, it was possible to obtain a few milligrams containing less than 1–2% of total impurities, also in agreement with the ES analyses performed on these samples. Those compounds were thus examined for their luminescence study, as in these cases proofs are obtained for their structure and purity.

Quite unexpectedly, the HPLC of the trimetallic compounds showed the presence of more than one product, in amounts sometimes larger than the expected complex. For example, for the heterometallic compound Rh_2 –Ru, as high as 50% of the bimetallic complex Rh–Ru were detected by HPLC, and for the trimetallic compound Rh– Ru_2 , the binuclear complex Ru_2 was present with a higher percentage than the Rh– Ru_2 . Moreover and quite amazingly, for the homonuclear complex Rh_3 , only the presence of a few percent of this compound was detected: the other percentages corresponded to the bimetallic product Rh_2 plus some starting material.

These HPLC data are hardly compatible with the FAB or electrospray analyses which indicated the presence of binuclear impurities in the trimetallic samples, but not in such amounts. This suggests significant decomposition during the HPLC analyses of the trimetallic complexes. Such an instability of the trimetallic compounds under HPLC conditions seems to be partly related to the presence of alcohol used for the elution. Indeed, as concluded by recording visible absorption spectra

(19) For the whole series of trimetallic compounds the characteristic pseudomolecular peaks ($\text{M} - \text{P}^-$, $\text{M} - 2\text{P}^-$ or $\text{M} - 3\text{P}^-$) are observed together with several other peaks corresponding to additional loss of uncharged PF_6 species and simultaneous addition of 16, 32, or 46 mass units. Similar peaks have already been observed in the FAB mass spectra previously obtained with these compounds. Loss of uncharged PF_6 corresponds either to a loss of a PF_6^- counterion with addition of one electron, or to the loss of a radical PF_6^\cdot ; addition of 16 and 32 mass units has been attributed to oxygen addition.¹⁶

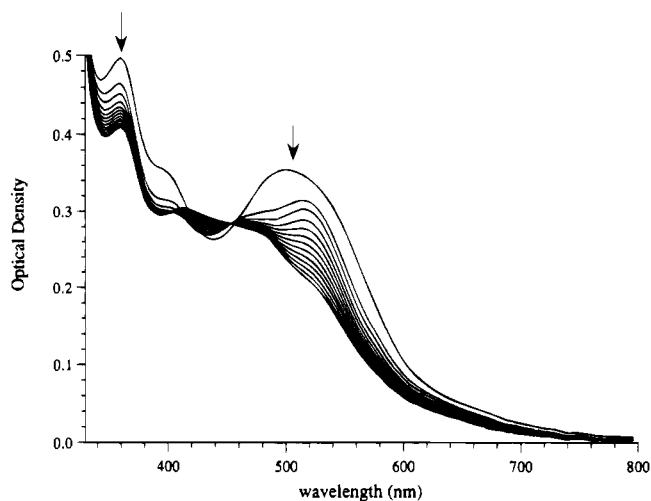


Figure 2. Visible absorption spectra recorded as a function of time for the heterotrimeric $[\text{Rh}(\text{PPY})_2]\text{HAT}[\text{Ru}(\text{BPY})_2]_2^{5+}$ complex dissolved in acetonitrile (2.5×10^{-5} M solution). The three first spectra were recorded at 5 min intervals and the following ones at 10 min intervals.

after different periods of dissolution of the complex in an organic solvent (Figure 2), the trinuclear compounds decompose rapidly in alcohols, acetonitrile, propionitrile, and butyronitrile, but are stable in water, dichloromethane, and propylene carbonate. It is probable that in acetonitrile (Figure 2) the compounds already decompose before the recording of the first absorption spectrum. Because of this decomposition, we have not been able to develop appropriate HPLC conditions that allow a careful examination of the purity of the trimetallic complexes, and consequently, their photophysical characteristics have not been investigated. The electrochemistry of the three trinuclear complexes is not exhibited either because these compounds are not enough soluble in the organic solvents in which they do not decompose (dichloromethane and propylene carbonate). On the other hand in acetonitrile where they are well soluble, the cyclic voltammetry reveals the presence of a mixture containing mainly mono- and bimetallic compounds and apparently no trimetallic complexes. This shows that decomposition is too fast in this solvent to determine the electrochemical characteristics. The electrochemical and photophysical studies are thus presented only for the binuclear Rh–Rh, Rh–Ru, and Ir–Ru compounds.

Electrochemistry. In table 2 are gathered the redox potentials of $[\text{Rh}(\text{PPY})_2]_2\text{HAT}^{2+}$, $[\text{Rh}(\text{PPY})_2]\text{HAT}[\text{Ru}(\text{BPY})_2]_2^{3+}$, and $[\text{Ir}(\text{PPY})_2]\text{HAT}[\text{Ru}(\text{BPY})_2]_2^{3+}$; those of the previously studied mono- and bimetallic compounds^{7,9b,12} are also included for comparison.

The reduction pathway characterizing the Rh–Rh homonuclear compound is complicated: only the first wave could be satisfactorily characterized because beyond -0.9 V/SCE the reduced products decompose as shown by the absence of corresponding anodic peaks during the reverse scans. In oxidation, a single irreversible one-electron wave is observed in the accessible potential range (until $+2$ V/SCE in acetonitrile) and appears at a more positive potential than for the corresponding monometallic species.

Both heteronuclear complexes Rh–Ru and Ir–Ru show a one-electron irreversible oxidation wave followed by a reversible oxidation process (Figure 3); by increasing the scan rate, the first oxidation wave for the Ir–Ru compound becomes however quasi-reversible (Table 2). Three reversible one-electron reductions are observed in the investigated potential range for the two heterobimetallic compounds.

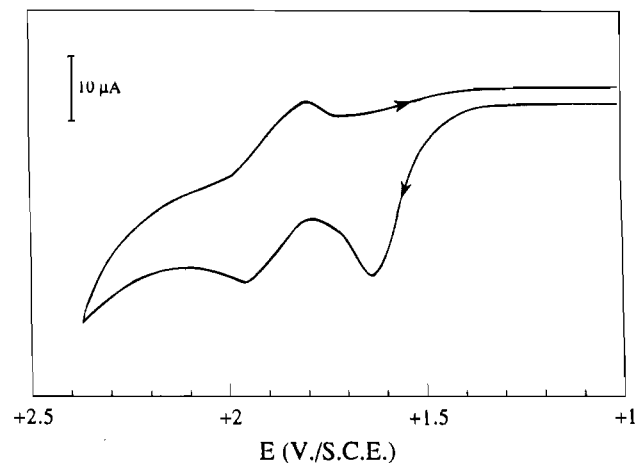


Figure 3. Cyclic voltammogram for the oxidation of the heteronuclear $[\text{Rh}(\text{PPY})_2]\text{HAT}[\text{Ru}(\text{BPY})_2]_2^{3+}$ complex (1 mM) at a Pt electrode in a nitrogen-purged acetonitrile solution (0.1 M in tetrabutylammonium hexafluorophosphate as supporting electrolyte), at room temperature; scan rate = 0.1 V/s.

UV–Visible Spectroscopy. Absorption. The absorption spectra of the bimetallic complexes and of their mono- and homobimetallic analogs are shown in Figure 4, and their main features are compiled in Table 3. The bimetallic heteronuclear Rh–Ru and Ir–Ru compounds display several absorption bands in the visible region attributed to CT (charge transfer) transitions whereas the homonuclear Rh_2 complex shows only a rather weak band or shoulder between 400 and 450 nm. Given the complexity of the spectra, we tried to obtain more data for one of the heterobimetallic compounds in the visible region: thus resonance Raman spectra were recorded for the Rh–Ru complex.

Resonance Raman. Figure 5a shows the resonance Raman (rR) spectra in water of the heteronuclear $[\text{Rh}(\text{PPY})_2]\text{HAT}[\text{Ru}(\text{BPY})_2]_2^{3+}$ compound at two excitation wavelengths (488 and 514 nm). The rR spectra of some reference compounds are also given for comparison purposes; the rR data recorded at the same irradiation wavelengths for $[\text{Ru}(\text{BPY})_2]\text{HAT}^{2+}$ are shown in Figure 5b, while the rR spectrum of $[\text{Ru}(\text{BPY})_2]_2\text{HAT}^{4+}$ previously obtained upon excitation at 514 nm is given in Figure 5c. Solubility problems in water have prevented us from recording the rR spectrum of $[\text{Rh}(\text{PPY})_2]_2\text{HAT}^{2+}$. For the monometallic $[\text{Rh}(\text{PPY})_2]\text{HAT}^+$, no rR data could be obtained because excitation in the absorption band (360 nm) resulted essentially in vibrations due to the quartz capillaries of the samples; therefore the Raman spectrum has been recorded for this monometallic Rh complex (Table S1). The explored frequency range covers $1200\text{--}1700\text{ cm}^{-1}$ which corresponds to C=C and C=N stretching frequencies.

Comparison of the data recorded for the heteronuclear complex with those of the reference compounds indicates clearly that in the heteronuclear compound the vibrations observed upon excitation at 514 nm originate from the bridging HAT. Indeed in the Rh–Ru rR spectrum almost all vibration bands have vanished except that at 1235 cm^{-1} , also observed for the homobimetallic $[\text{Ru}(\text{BPY})_2]_2\text{HAT}^{4+}$ compound (Figure 5c). For this latter complex the 1235 cm^{-1} band intensification had been attributed to an important enhancement of the pyrazine-like vibrations by multicomplexation.^{10a} In addition it should be noted that in the rR spectra of the monometallic $[\text{Ru}(\text{BPY})_2]\text{HAT}^{2+}$ upon excitation at 514 and 488 nm, BPY vibration bands can be distinguished, which in contrast is not the case for the heteronuclear Rh–Ru compound at 514 nm nor for the homobimetallic Ru–Ru complex. Consequently the

Table 2. Oxidation and Reduction Potentials in Acetonitrile Containing 0.1 M Tetrabutylammonium Hexafluorophosphate^e

complex	oxidn potential, V (vs SCE)		redn potential, V (vs SCE)			
	1	2	1	2	3	4
Ru(BPY) ₂ HAT ²⁺ ^a	+1.56 (r)		-0.84 (r)	-1.43 (r)		
Rh(PPY) ₂ HAT ⁺ ^b	+1.59 (ir)		-0.88 (r)	-1.49 (r)		
Ir(PPY) ₂ HAT ⁺ ^b	+1.43 (ir) ^d		-0.75 (r)	-1.37 (r)		
[Rh(PPY) ₂] ₂ HAT ²⁺	+1.81 (ir)		-0.44 (r)	-0.91 (ir)	-1.19 (ir)	-1.49 (ir)
[Rh(PPY) ₂] ₂ HAT[Ru(BPY) ₂] ³⁺ ^c	+1.63 (ir)	+1.88 (r)	-0.43 (r)	-1.02 (r)	-1.41 (r)	
[Ir(PPY) ₂] ₂ HAT[Ru(BPY) ₂] ³⁺ ^c	+1.42 (ir) ^d	+1.73 (r)	-0.41 (r)	-1.02 (r)	-1.47 (r)	-1.66 (ir)
[Ru(BPY) ₂] ₂ HAT ⁴⁺ ^a	+1.53 (r)	+1.78 (r)	-0.49 (r)	-1.06 (r)		

^a References 7 and 9b. ^b Reference 12. ^c The presence of minor impurities (5% of Ru(BPY)₂HAT²⁺ and [Rh/Ir(PPY)₂Cl]₂) in the heterometallic samples does not affect the cyclic voltammetric results. ^d When the scan rate increases (from 0.1 to 1 V/s), a very weak cathodic peak is detected on the reverse scan, which indicates a quasi-reversibility of the wave. In that case, the potential value given in the table corresponds to the average of E_{pa} and E_{pc} . ^e Scan rate = 0.1 V/s; r = reversible and ir = irreversible; all values are ± 0.01 V. For the reversible waves, the anodic and cathodic peak currents ratios are quasi-equal to 1 whereas the peak separation fluctuates between 60 and 100 mV (ohmic loss is likely to be responsible for this deviation from the theoretical value). For the totally irreversible waves, only the anodic or cathodic peak potentials (E_{pa} or E_{pc}) are mentioned.

rR results of the heterobimetallic complex Rh–Ru show that in the absorption region from 490 nm toward longer wavelengths, the CT transition toward the bridging HAT has become much more important than toward the BPY ligand. From these data, we thus conclude that the addition of a Rh(III) moiety to [Ru(BPY)₂]₂HAT²⁺ has the same effect on the bridging ligand vibrations as the addition of a Ru(II) moiety. From the available data it is however difficult to conclude whether the CT toward the HAT bridge ($\lambda > 490$ nm) originates from a Ru or a Rh center.

Emission. In Table 4 are collected the luminescence data recorded at room temperature in CH₂Cl₂ and propylene carbonate for the bimetallic heteronuclear complexes and for the corresponding monometallic units for comparison purposes.²⁰ No luminescence data are available at low temperature in a rigid matrix of organic solvents because the binuclear complexes decompose very slowly in these solvents, which leads to contamination by traces of monometallic impurities and has prevented us from recording reliable 77 K emission spectra. No emission could be observed for the homonuclear compound [Rh(PPY)₂]₂HAT²⁺ at room temperature in fluid solution.

The corrected excitation spectrum recorded in dichloromethane for the heterobimetallic Rh–Ru complex ($\lambda_{exc} = 320$ – 600 nm; $\lambda_{em} = 730$ nm) corresponds reasonably well to the absorption spectrum.²¹ For the Ir–Ru complex the excitation spectrum shows a poor quality because of the low emission quantum yield; however, a comparison of the excitation spectrum with the absorption data would indicate a more intense contribution of the most bathochromic band (i.e. between 500 and 590 nm) in the excitation spectrum.

Discussion

Characterization, Stability and Purity of the Complexes.

The previously obtained FAB results¹⁶ and the ESMS data give

- (20) When the [Rh(PPY)₂]₂HAT[Ru(BPY)₂]³⁺ sample is not purified several times as indicated above (i) the emission spectrum depends upon the excitation wavelength and two maxima appear at 720 nm and 770 nm (in propylene carbonate; non corrected) by excitation between 410 and 470 nm, and (ii) the luminescence decay does not correspond to a single exponential; the long decay component corresponds to the blue emission. These observations are in accordance with the presence of the monometallic Ru(II) complex as emitting impurity, as concluded unambiguously from the HPLC data.
- (21) The absorption maxima ($\lambda_{max} = 362$ nm, 408 nm, 462 nm and 510 nm in dichloromethane) coincide with the corresponding maxima measured from the excitation spectrum ($\lambda_{max} = 365$, 410, 455, and 513 nm). It seems however that the relative intensities of the bands centered at ~ 410 nm and ~ 455 nm are slightly higher in the excitation spectrum than in the absorption spectrum: this small distortion could originate from traces of monometallic [Ru(BPY)₂]₂HAT²⁺ still present in the sample.

unambiguous support to the proposed structure for the bimetallic compounds Rh–Rh, Rh–Ru, and Ir–Ru. Moreover, for these compounds, conditions were found where only parent peaks ($M - P^-$, $M - 2P^-$) were present, which rules out the presence of monometallic impurities. These results are in total agreement with the HPLC analyses of the bimetallic complexes which do not reveal the presence of impurities when the products are chromatographed several times and with small amounts, especially for the heteronuclear complexes.

In contrast, all the trimetallic complexes (homo- and heteronuclear) show very complicated chromatograms as compared to the bimetallic compounds; besides, the expected product is not always detected in majority proportions. Even more surprising, for the trimetallic [Rh(PPY)₂]₃HAT³⁺ complex for example, only 3% is detected by HPLC. This is particularly unexpected if we consider the previously obtained FAB results¹⁶ and the ESMS data presented in Table 1. The ES mass spectrum obtained at low cone voltage with Rh₃ contains three pseudomolecular peaks ($m/z = 1757.9$, 805.9, and 489.7) corresponding to the loss of one, two, and three PF₆⁻ ions, which is in accordance with the expected product. On the other hand peaks that correspond to [Rh(PPY)₂]₂HAT²⁺ and [[Rh(PPY)₂]₂HAT²⁺PF₆⁻]⁺ are also present in the ES spectrum recorded at reduced cone voltage; these peaks could originate either from a fragmentation of the trimetallic complex or from contamination by the bimetallic Rh₂ compound. However, taking into account the low accelerating voltage conditions ($V_c = 10$ V) and the absence of any Rh(PPY)₂⁺ fragment, the hypothesis of the presence of a bimetallic impurity seems more probable. Nevertheless, in spite of a contamination by a Rh₂ species, it is clear from relative peak intensities that the expected Rh₃ complex represents more than 3% of the analyzed sample (on the basis of a similar detector response in electrospray for the [Rh(PPY)₂]_nHATⁿ⁺ ($n = 1, 2, 3$) series). The same type of conclusion can be reached from the ESMS data obtained for the other trimetallic complexes.

Consequently a partial decomposition on the HPLC column, partly due to decomposition in MeOH, is probable for these compounds. Comparison with previously studied homonuclear Ru–HAT compounds,^{7,9b} for which HPLC analyses were not destructive, suggests that the trimetallic complexes based on the bridging ligand HAT, containing at least one Rh(PPY)₂⁺ moiety, are much more sensitive to decomposition than trimetallic homonuclear Ru–HAT compounds. This is probably due to the high π -deficient character of HAT.

Electrochemistry. As mentioned above the homonuclear Rh–Rh complex displays a complicated reduction pattern. Nevertheless, considering the relative oxidation power of the

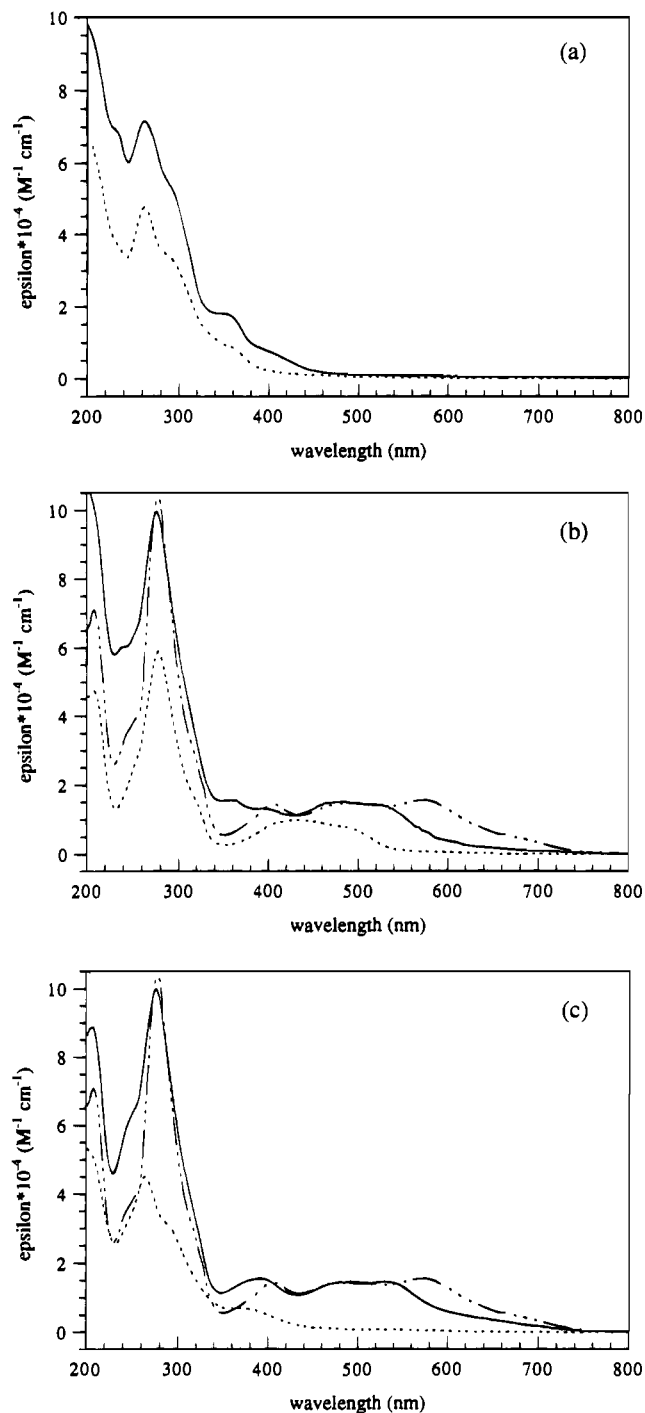


Figure 4. UV-Visible absorption spectra of aqueous solutions of (a) Rh(PPY)₂HAT⁺ (---) and [Rh(PPY)₂]₂HAT²⁺ (—), (b) Ru(BPY)₂HAT²⁺ (---), [Rh(PPY)₂]₂HAT[Ru(BPY)₂]³⁺ (—), and [Ru(BPY)₂]₂HAT⁴⁺ (---), and (c) Ir(PPY)₂HAT⁺ (---), [Ir(PPY)₂]₂HAT[Ru(BPY)₂]³⁺ (—), and [Ru(BPY)₂]₂HAT⁴⁺ (---).

ligands HAT and PPY, the first electron added should be localized on the bridging HAT ligand. This is in agreement with the fact that the PPY reduction has only been observed at potentials more negative than -2.4 V/SCE for Rh(PPY)₂BPY⁺ in *N,N*-dimethylformamide at -54 °C.²² Additional evidence in support of this assignment is found by comparing the position of the first reduction wave in [Rh(PPY)₂]₂HAT²⁺ (-0.44 V/SCE) with that of [Ru(BPY)₂]₂HAT⁴⁺ (-0.49 V/SCE) for which it was concluded that the first electron was also added

Table 3. Absorption Data

complex	λ_{\max} of absorption, nm			$10^{-4} \epsilon, ^a$ M ⁻¹ cm ⁻¹
	H ₂ O	prop carb	CH ₂ Cl ₂	
Ru(BPY) ₂ HAT ²⁺	207 ^c	275 ^b	258 ^b	4.5 ^c
	277 ^c	282	280	5.9 ^c
	432 ^c	422	425	1.0 ^c
	484 ^{b,c}	478 ^b	468 ^b	
Rh(PPY) ₂ HAT ⁺	214 ^d			
	266 ^d	265	264	4.65 ^d
	290 ^{b,d}	285 ^b	288 ^b	
	354 ^{b,d}	355 ^b	354 ^b	0.92 ^d
Ir(PPY) ₂ HAT ⁺	264 ^d	262	266	4.5 ^d
		282 ^b	290 ^b	
	376 ^d	368	370	0.7 ^d
[Rh(PPY) ₂] ₂ HAT ²⁺	220 ^b			6.8
	260	262	266	7.1
	290 ^b	290 ^b	285 ^b	
	360	356 ^b	354	1.8
	390 ^b	388 ^b	385 ^b	
[Rh(PPY) ₂] ₂ HAT[Ru(BPY) ₂] ³⁺	230 ^b	250		
	276	280	280	9.95
	354 ^b	365	362	1.52
	400	405	408	1.25
	468	470 ^b	462 ^b	1.54
	528	515	510	1.31
[Ir(PPY) ₂] ₂ HAT[Ru(BPY) ₂] ³⁺	246 ^b	250 ^b	260 ^b	
	276	278	276	9.99
	390	398	398	1.54
	480	466 ^b	468 ^b	1.42
	530	524	530	1.45
[Ru(BPY) ₂] ₂ HAT ⁴⁺	206 ^c			7.4 ^c
	243 ^{b,c}			
	252 ^{b,c}			
	276 ^c	280	280	10.5 ^c
	405 ^c	414	414	1.4 ^c
	490 ^c	466 ^b	462	1.4 ^c
	572 ^c	554	1.5 ^c	

^a Extinction coefficient determined in H₂O. ^b Shoulder. ^c Reference 7. ^d Reference 12.

on the bridging HAT.^{7,9b} Moreover this first reduction wave appears also at a more anodic potential (440 mV) than in the case of the monometallic [Rh(PPY)₂]₂HAT⁺ unit. This result appears to be consistent with a strong stabilization of the lowest unoccupied π^* molecular orbital localized on the bridging ligand, due to the addition of a second electron withdrawing Rh(PPY)₂⁺ moiety. A similar effect has already been observed in the series of homonuclear compounds [Ru(BPY)₂]_nHAT²ⁿ⁺ ($n = 1, 2, 3$).^{7,9b}

The second reduction wave characterizing the bimetallic [Rh(PPY)₂]₂HAT²⁺ complex (-0.91 V/SCE) is also anodically shifted as compared to the corresponding wave in the monometallic unit (-1.49 V/SCE) where it had been assigned to a second reduction of the HAT ligand.¹² Consequently, the second reduction for the bimetallic Rh compound should also correspond to the addition of a second electron to the bridging HAT. As this second wave is irreversible, the bireduced Rh–Rh compound decomposes probably into two other products that are reduced at more negative potentials; one of them (-1.49 V/SCE) might correspond to monoreduced Rh(PPY)₂HAT⁺.

The oxidation behavior of [Rh(PPY)₂]₂HAT²⁺ is characterized by a single irreversible wave in the accessible potential range. In the previously studied monometallic Rh compound, the highest occupied molecular orbital (HOMO) had been assigned to a Rh–C σ -bonding orbital, resulting from a strong admixture of a σ -bonding PPY orbital with a $d\sigma(e_g)$ Rh orbital;¹² therefore, the electrons which occupy the HOMO may be regarded as originating from the carbanion formed by loss of a proton when

(22) Oshawa, Y.; King, K. A.; DeArmond, M. K.; Hanck, K. W.; Watts, J. R. *J. Phys. Chem.* **1987**, *91*, 1047.

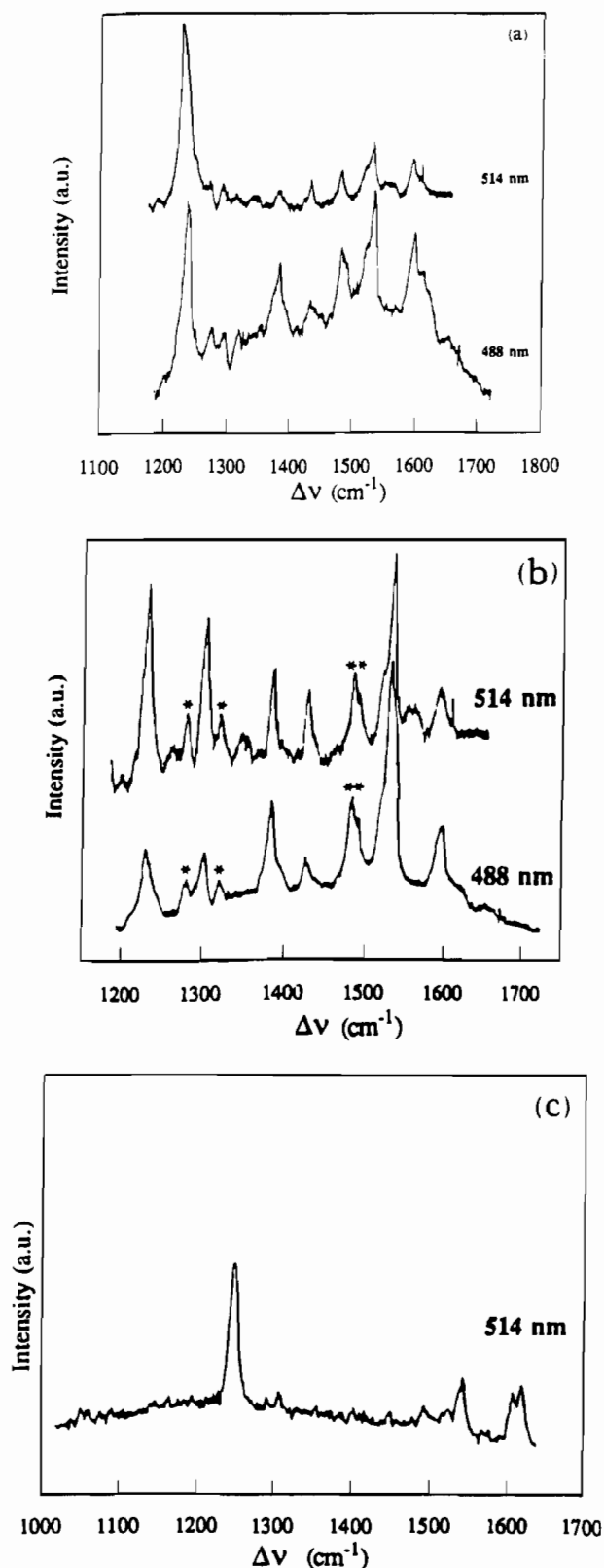


Figure 5. Resonance Raman spectra recorded in water under irradiation at 488 nm and 514 nm for (a) $[\text{Rh}(\text{PPY})_2]\text{HAT}[\text{Ru}(\text{BPY})_2]^{3+}$, (b) $[\text{Ru}(\text{BPY})_2]\text{HAT}^{2+}$, and (c) $[\text{Ru}(\text{BPY})_2]_2\text{HAT}^{4+}$. For Figures 5b and 5c a single asterisk denotes BPY vibrations; two asterisks: BPY or HAT vibrations; no asterisk: HAT vibrations. For the heteronuclear compound (Figure 5a), all the vibrations (488 nm) cannot clearly be identified because no reference rR spectra were available for the homonuclear Rh compounds (see results).

the metal-carbon bond is formed. As a result, the irreversible oxidation wave observed for $[\text{Rh}(\text{PPY})_2]\text{HAT}^+$ had been attributed to the removal of an electron localized on a $L\sigma-d\sigma$

Table 4. Emission Data

complex	prop carb		CH_2Cl_2	
	$\lambda_{\text{max}},^a$ nm	τ , ns	$\lambda_{\text{max}},^a$ nm	τ , ns
$\text{Ru}(\text{BPY})_2\text{HAT}^{2+}$	690	390	676	470
$\text{Rh}(\text{PPY})_2\text{HAT}^+$	625 ^b	120 ^b	620	200
$\text{Ir}(\text{PPY})_2\text{HAT}^+$	710 ^b	<10 ^b	716	<10
$[\text{Rh}(\text{PPY})_2]\text{HAT}[\text{Ru}(\text{BPY})_2]^{3+}$	770	100	735	180
$[\text{Ir}(\text{PPY})_2]\text{HAT}[\text{Ru}(\text{BPY})_2]^{3+}$	790	<10	760	<10
$[\text{Ru}(\text{BPY})_2]_2\text{HAT}^{4+}$	775	473	755	1070

^a Noncorrected for the photomultiplier response. ^b Reference 12.

bonding orbital, and irreversibility was thought to be the result from subsequent cleavage of the Rh-C bond. The irreversible nature of the oxidation wave characterizing the bimetallic Rh-Rh complex suggests a similar assignment. This implies that the nature of the HOMO in $[\text{Rh}(\text{PPY})_2]_2\text{HAT}^{2+}$ is unchanged with respect to the monometallic unit.

It seems a priori surprising that the addition of a second Rh-(PPY)₂⁺ moiety to the monometallic $[\text{Rh}(\text{PPY})_2]\text{HAT}^+$ leads to an important anodic shift of the oxidation process whereas this is not the case when one or two $\text{Ru}(\text{BPY})_2^{2+}$ moieties are added to $[\text{Ru}(\text{BPY})_2]\text{HAT}^{2+}$.⁷ The totally irreversible character of the oxidative waves for the mono- and bimetallic Rh compounds has however to be taken into account. The absence of cathodic peak during the reverse scan indicates that the electron transfer process is followed by a fast chemical reaction. In that case, the anodic peak potential is given by²³

$$E_{\text{pa}} = E_{\text{ox}} - 0.78 \cdot RT/nF + \ln \lambda \cdot RT/2nF \quad (1)$$

with λ (dimensionless kinetic parameter) = $k_{\text{react}}/\nu(RT/nF)$ ($\lambda > 5$), where E_{ox} stands for the oxidation redox potential, F the Faraday constant, n the number of electrons involved in the electrochemical process, R the ideal gas constant, T the temperature, k_{react} the chemical reaction rate constant of the species generated by oxidation, and ν the scan rate.

Equation 1 shows that (i) the anodic peak potential E_{pa} is anodically shifted as compared to the redox oxidation potential E_{ox} and (ii) this anodic shift increases with k_{react} . Thus the E_{ox} value for the monometallic $[\text{Rh}(\text{PPY})_2]\text{HAT}^+$ should be less positive than its measured E_{pa} value.²⁴ Moreover the anodic shift of E_{pa} from the mononuclear $[\text{Rh}(\text{PPY})_2]\text{HAT}^+$ to the bimetallic $[\text{Rh}(\text{PPY})_2]_2\text{HAT}^{2+}$ would indicate that decomposition of the oxidized bimetallic Rh₂ complex is faster than transformation of the oxidized monometallic Rh complex, which seems reasonable. This shift would thus not suggest a priori a different energy level of the $L\sigma-d\sigma$ orbital in the two Rh compounds.

The heteronuclear complexes $[\text{Rh}(\text{PPY})_2]\text{HAT}[\text{Ru}(\text{BPY})_2]^{3+}$ and $[\text{Ir}(\text{PPY})_2]\text{HAT}[\text{Ru}(\text{BPY})_2]^{3+}$ display three reversible reduction waves in the accessible potential range, followed by ill-resolved irreversible waves. For similar reasons to those discussed above, the two first reductions should involve antibonding π^* molecular orbitals centered on the bridging HAT

(23) Bard, A. J.; Faulkner, L. R. in *Electrochemical Methods*; J. Wiley & Sons: New York, 1980.

(24) As the anodic peak potential E_{pa} for the mononuclear $[\text{Rh}(\text{PPY})_2]\text{HAT}^+$ compound appears approximately at the same value as the redox oxidation potential E_{ox} of $[\text{Ru}(\text{BPY})_2]\text{HAT}^{2+}$, and taking into account that the E_{ox} should be less positive than the measured E_{pa} (eq 1), the $L\sigma-d\sigma$ orbital of $[\text{Rh}(\text{PPY})_2]\text{HAT}^+$ would be located above the $d\pi$ orbital of $[\text{Ru}(\text{BPY})_2]\text{HAT}^{2+}$. On the other hand, despite the fact that the reduction potentials of $[\text{Rh}(\text{PPY})_2]\text{HAT}^+$ and $[\text{Ru}(\text{BPY})_2]\text{HAT}^{2+}$ are similar, this conclusion would not mean that the monometallic Rh complex should luminesce more bathochromically than the monometallic Ru compound. Indeed the linear spectroelectrochemical correlations between the emission energies and the $E_{\text{ox}} - E_{\text{red}}$ values are certainly different for the Rh and Ru complexes.

ligand. This attribution seems further confirmed by the similar values observed for the corresponding reductions of the previously studied bimetallic $[\text{Ru}(\text{BPY})_2]_2\text{HAT}^{4+}$ compound. The third reduction process is attributed to a BPY-based process.

The first oxidation wave of the heterobimetallic complex Rh–Ru is totally irreversible and slightly more anodic than the corresponding waves of the monometallic $[\text{Ru}(\text{BPY})_2]\text{HAT}^{2+}$ and $[\text{Rh}(\text{PPY})_2]\text{HAT}^+$ compounds. On the basis of its irreversible character this wave could be attributed to a rhodium-centered oxidation process involving a Rh–C σ -bonding orbital; the second reversible oxidation would correspond to removal of a Ru-centered electron from a new and unknown species produced by the first oxidation step. This attribution would imply that emission in this Rh–Ru compound would originate from a Rh–HAT SBLCT (σ -bond to ligand charge transfer) excited state.

Another hypothesis however could be considered. Indeed the first irreversible wave could also be attributed to the oxidation of the Ru moiety as it is only slightly more anodic than the oxidation of $[\text{Ru}(\text{BPY})_2]\text{HAT}^{2+}$. This anodic shift could be attributed to the irreversible character of the wave. The irreversibility would result in this case from the fact that the electrochemically generated Ru(III) center would oxidize the Rh–C bond, regenerating Ru(II). The second oxidative wave would in such conditions correspond to the reversible oxidation of the same Ru(II) center of a modified bimetallic complex. According to this second hypothesis, the Ru centered $d\pi$ level in the Rh–Ru complex would be higher than the Rh–C $L\sigma-d\sigma$ level and consequently the lowest energy excited state would correspond to a Ru–HAT MLCT (metal to ligand charge transfer) state.

For the Ir–Ru heterometallic complex only one hypothesis could be proposed for the attribution of the first irreversible oxidation wave. Indeed, as the oxidation appears at the same potential as for the monometallic $[\text{Ir}(\text{PPY})_2]\text{HAT}^+$ complex, and as this potential is significantly less anodic than those for the oxidations of the monometallic $[\text{Ru}(\text{BPY})_2]\text{HAT}^{2+}$ and of the bimetallic $[\text{Ru}(\text{BPY})_2]_2\text{HAT}^{4+}$, the first irreversible wave cannot correspond to the oxidation of the Ru(II) center. Instead it should be attributed to the oxidation of the Ir(III) center. The quasi reversibility of the oxidation wave at high scan rate, also observed for the monometallic $[\text{Ir}(\text{PPY})_2]\text{HAT}^+$ compound, would indicate that the electron involved in the oxidation process originates from an admixture of Ir–C σ -bonding and Ir $d\pi$ orbitals very close in energy.¹² Consequently for the Ir–Ru complex, the Ir–C $L\sigma-d\sigma$ and Ir $d\pi$ orbitals should lie above the Ru $d\pi$ level, and emission should originate from the Ir–HAT SBLCT or MLCT excited state.

Absorption and Emission Spectroscopy. The intense absorption bands in the UV region of the spectrum ($\lambda < 350$ nm) for the homobimetallic $[\text{Rh}(\text{PPY})_2]_2\text{HAT}^{2+}$ are attributed to ligand localized $\pi-\pi^*$ transitions. In addition to these LC transitions, the spectrum for this bimetallic complex displays two other bands or shoulders, one of which extends into the visible region. The corresponding extinction coefficients are indicative of CT (charge transfer) transitions. On the basis of the electrochemical results and according to the recently reported behavior of the monometallic analog, the lowest energy absorption is assigned to a SBLCT transition, corresponding to the promotion of an electron from the $L\sigma-d\sigma$ bonding orbital to the lowest unoccupied π^* acceptor orbital of the bridging ligand HAT.

The red shift observed in the visible for this lowest energy transition from the mono- to the bimetallic compound is consistent with stabilization of the bridging ligand localized π^*

orbitals by complexation of two metal centers. The absorption band centered around 360 nm would correspond either to a $d\pi-\pi^*$ Rh–HAT MLCT transition (if not mixed with the SBLCT transition in the visible), or to a Rh–PPY MLCT transition.

No room temperature emission is detected for this homonuclear Rh–Rh compound in the investigated solvents. This contrasts with the monometallic unit $[\text{Rh}(\text{PPY})_2]\text{HAT}^+$ ¹² and with the bimetallic $[\text{Ru}(\text{BPY})_2]_2\text{HAT}^{4+}$ ^{7,9b} complex that luminesce from an SBLCT and an MLCT excited state respectively. On the basis of the cyclic voltammetric results discussed above combined with the absorption assignments, it is reasonable to assume that the lowest excited state of $[\text{Rh}(\text{PPY})_2]_2\text{HAT}^{2+}$ corresponds also to an SBLCT state; the absence of luminescence probably suggests a higher efficiency of non radiative deactivation processes, such as Rh–C bond cleavages, as compared to the monometallic $[\text{Rh}(\text{PPY})_2]\text{HAT}^+$ unit.

Apart from the $\pi-\pi^*$ transitions displayed in the UV region of the absorption spectra of both heteronuclear Rh–Ru and Ir–Ru complexes, several broad bands appear in the visible range. The high extinction coefficients of these bands are indicative of CT transitions. Different kinds of CT transitions are likely to occur depending upon the nature of the metal and the ligand involved. Transitions towards the bridging ligand (Ru–HAT MLCT, Rh/Ir–HAT SBLCT and Rh/Ir–HAT MLCT) are expected to show a bathochromic shift as compared to the corresponding transitions displayed by the monometallic complexes $[\text{Ru}(\text{BPY})_2]\text{HAT}^{2+}$, $[\text{Rh}(\text{PPY})_2]\text{HAT}^+$, and $[\text{Ir}(\text{PPY})_2]\text{HAT}^+$. In contrast, transitions involving ancillary ligands are not supposed to be much affected with respect to similar transitions occurring in the monometallic units.

The assignment of the ligand involved in the lowest energy charge transfer band ($\lambda = 490$ to 580 nm) for the Rh–Ru compound can be performed on the basis of the reduction behavior and of the resonance Raman experiments. According to cyclic voltammetry, the lowest unoccupied molecular orbital corresponds to a HAT-centered π^* orbital; this fact supports attribution of the lowest energy transition to a CT band involving the bridging HAT ligand. In accordance with this conclusion, the rR data obtained for the bimetallic Rh–Ru complex upon excitation in the visible region ($\lambda > 490$ nm) indicate clearly the absence of CT bands to a BPY or a PPY ligand and the presence of a CT transition to the HAT. Whether this transition corresponds to a Rh–HAT SBLCT or a Ru–HAT MLCT cannot be easily concluded. Indeed no good reference data are available for the rR spectra of the Rh–HAT compounds. Moreover the oxidation results do not furnish supplementary information because of the two possible attributions for the first oxidation wave characterizing the Rh–Ru complex. The absorption band centered around 400 nm could be attributed to a Ru–BPY MLCT transition, by analogy to previously reported assignments for the homonuclear $[\text{Ru}(\text{BPY})_2]_2\text{HAT}^{4+}$.^{7,9b}

The heteronuclear Rh–Ru complex shows an emission band centered at ~ 770 nm (non corrected), with a 100 ns lifetime in propylene carbonate. According to the absorption assignments and as outlined before from the electrochemical data, the luminescence could be attributed either to a Ru–HAT ³MLCT or to a Rh–HAT ³SBLCT emission.²⁵ The corrected excitation spectrum recorded for this heteronuclear complex at 730 nm in CH_2Cl_2 corresponds reasonably well to its absorption spectrum,

(25) No further argument which would allow one to choose between these luminescence assignments can be found at the present stage. Indeed the structure of the luminescence band at low temperature, different for SBLCT and MLCT emissions, cannot be used as supplementary information as it was not possible to record low temperature emission spectra (see Results).

which indicates the occurrence of an efficient energy transfer from one metallic unit toward the other moiety.

For the Ir–Ru complex, the electrochemical data indicate that the closely lying Ir–C σ -bonding and Ir $d\pi$ orbitals are located above the Ru-centered $d\pi$ level. This suggests the presence of Ir–HAT SBLCT mixed with Ir–HAT MLCT absorption bands, responsible for the lowest energy absorption. On the basis of these considerations the luminescence from the Ir–Ru compound should be regarded as a result of a strong admixture of Ir–HAT 3 SBLCT and 3 MLCT behavior, also characteristic of the monometallic [Ir(PPY)₂]HAT⁺ complex. The excitation spectrum exhibits a relatively more important contribution of the lowest energy band (500–590 nm): this would suggest that the energy transfer from the Ru fragment to the Ir unit is not total.

Acknowledgment. The authors would like to thank Prof. J. Mc Garvey (Queen's University of Belfast) who made possible the resonance Raman measurements, Dr. M. Demeunynck who contributed to the HPLC tests, and Prof. A. van Dorsselaer and Dr. E. Leize for the ESMS measurements. They are grateful to the "Communauté Française de Belgique" (ARC 91/96-149) for financial support of this work. P.D. and I.O. thank the NATO and the FNRS (Fonds National de la Recherche Scientifique) for a fellowship.

Supporting Information Available: Raman data recorded for the [Rh(PPY)₂]HAT⁺ complex (Table S1) (1 page). Ordering information is given on any current masthead page.

IC940827S